



Babanin, A. V., Ganopolski, A., Phillips, W. R. C. (2009). Wave-induced upper-ocean mixing in a climate model of intermediate complexity

Originally published in *Ocean Modelling*, 29 (3), 189-197

Available from:

<http://dx.doi.org/10.1016/j.ocemod.2009.04.003>

Copyright © 2009 Elsevier Ltd. All rights reserved.

This is the author's version of the work. It is posted here with the permission of the publisher for your personal use. No further distribution is permitted. If your library has a subscription to this journal, you may also be able to access the published version via the library catalogue.



# Wave-induced upper-ocean mixing in a climate model of intermediate complexity

Alexander V. Babanin, Andrey Ganopolski, William R.C. Phillips

## Abstract

Climate modelling, to a great extent, is based on simulating air–sea interactions at larger scales. Smallscale interactions and related phenomena, such as wind-generated waves and wave-induced turbulence are sub-grid processes for such models and therefore cannot be simulated explicitly. In the meantime, the waves play the principal role in the upper-ocean mixing. This role is usually parameterized, mostly to account for the wave-breaking turbulence and to describe downward diffusion of such turbulence. The main purpose of the paper is to demonstrate that an important physical mechanism, that is the ocean mixing due to waves, is presently missing in the climate models, whereas the effect of this mixing is significant. It is argued that the mixing role of the surface waves is not limited to the mere transfer of the wind stress and energy across the ocean interface by means of breaking and surface currents. The waves facilitate two processes in the upper-ocean which can deliver turbulence to the depths of the order of 100 m directly, rather than diffusing it from the surface. The first process is due to capacity of the waves to generate turbulence, unrelated to the wave breaking, at all depths where the wave orbital motion is significant. The second process is Langmuir circulation, triggered by the waves. Such wave-controlled mixing should cause seasonal variations of the mixed-layer depth, which regulates the thermodynamic balance between the ocean and atmosphere. In the present paper, these variations are parameterized in terms of the global winds. The variable mixed-layer depth is then introduced in the climate model of intermediated complexity CLIMBER-2 with a purpose of reproducing the pre-industrial climate. Comparisons are conducted with the NRL global atlas of the mixed layer, and performance of the wave-mixing parameterisations was found satisfactory in circumstances where the mixing is expected to be dominated by the wind-generated waves. It is shown that as a result the seasonal temperature modulations and extremes are significantly enhanced. This effect combines with changes in the global pressure patterns and leads to large localized alterations of precipitation. Possible future scenarios are also simulated. Finally, importance of the wave-mixing physics and its relevance for the general circulation models is discussed.

**Keywords:** Climate modeling, Air–sea interactions, Wind-generated waves, Wave-induced turbulence, Langmuir circulation, Mixed-layer depth

## 1. Introduction

Climate modelling, to a great extent, is based on simulating air–sea interactions. The solar energy crosses the atmosphere–ocean interface at least three times before it comes to rest (e.g. Donelan, 1990): first, the near-surface water layer is heated, then it forms the atmospheric circulation, and finally the winds generate the waves which dissipate their energy and pass their momentum on to the ocean turbulence and currents. The processes involved cover the range of scales from global in space and inter-centennial in time (climate) down to the waves and turbulence (meters and seconds or less). While it is tempting to allocate different physics to separate large-scale and small-scale processes, in general the continuous and decoupling exists as a simplifying

means of analysis, justified in many cases, but likely to fail or produce biases in others. In short, the processes highlight a cascade of energy through an almost continuous spectrum of scales. In computing such events, however, there are limitations to the range of length and time scales that can be included. This means that at some point the cascade must be halted and that processes with scales smaller than the cutoff, namely sub-grid processes, must be ignored, parameterized or dynamically modelled. In doing so, large and small-scale processes are essentially decoupled, an unfortunate but necessary occurrence not directly based on first principles. Our only recourse to this truncation is to include as much key physics as possible in the sub-grid model. Thus, the purpose of the present work is to include more physics in our model of the mixed layer, specifically two mixing processes that act to deepen it, these being wave-induced turbulence and Langmuir circulation. We further allow for the fact that the depth of the mixed layer may vary. Both mechanisms are expressed in parameterized form.

Small-scale interactions and related phenomena, such as wind-generated waves and wave-induced turbulence are sub-grid processes for climate models and therefore cannot be simulated by them explicitly. In the meantime, the waves, at the very least, modulate all the air–sea exchanges, but they also play the primary role in the upper-ocean mixing which fast-tracks the thermodynamic balance between the atmosphere and the ocean. This role is often overlooked in the large-scale models, and the wind is parameterized to directly drive the dynamics of the upper-ocean, i.e. wind stress provides momentum flux to the ocean surface and that flux is then diffused down by means of parameterized turbulence. The dominant part of the wind stress, however, is supported by the flux of momentum from wind to waves (e.g. Kudryavtsev and Makin, 2002). This means that, before the momentum is received by the upper-ocean in the form of turbulence and mean currents, and thus enters the further cycle of air–sea interaction, it goes through a stage of wave motion. In the course of events, the waves only accumulate a small fraction of the energy and momentum received (3–4%, Donelan, 1998), the rest is dissipated locally through the wave breaking. Therefore, if the only role of the waves was to transfer the momentum under the ocean skin, the overall approach would be acceptable.

However, apart from injecting the turbulence by means of the breaking to the depths comparable with the wave height (i.e. the order of meters (e.g. Terray et al., 1996; Babanin et al., 2005)), the wave motion can directly affect or influence the upper-ocean mixing and other processes down to the depths of the order of 100 m. Since 2–3 m of the sea water has the same heat capacity as the entire atmosphere (e.g. Gill, 1982; Soloviev and Lukas, 2006), then misprediction of the mixed-layer depth (MLD) may undermine accuracy of the modelling.

The wave-related processes which can deliver turbulence directly to the depth of the order of 100 m, instead of diffusing it from the top, are two. The first mechanism is due to turbulence induced by the wave orbital motion, which is unrelated to the breaking (Babanin, 2006; Babanin and Haus, 2009). This turbulence should persist at any depth where the wave motion is significant, and therefore, even within traditional  $k - \epsilon$  mixing schemes, will provide an additional turbulent source which is also distributed over the depth. Potentially, it may even facilitate the mixing across thermocline.

The second process is Langmuir circulation (Langmuir, 1938; Smith, 1992; Phillips, 2001, 2002, 2005) (see also Section 2.2) or more precisely Langmuir turbulence, which is characterized by a spectrum of Langmuir circulation (McWilliams et al., 1997). These circulations are a consequence of an instability resulting from the waves interacting with both themselves and a weak shear brought on by the wind (Craik and Leibovich, 1976; Phillips, 1998). Moreover they can form in tens of minutes after an increase in wind strength and continue for days, long after the wind has subsided. During that period their spacing can grow from millimeters to kilometers (Phillips, 2001; Thorpe, 2004) but, because they are dependent for their existence on the wave-induced drift (Stokes drift in the case of irrotational waves), their depth is restricted to circa that of the wavelength of the dominant surface waves. Their rate of rotation is necessarily slow (of the order of cm/s); nevertheless, Langmuir circulations provide a means to advect turbulence kinetic energy abundant in surface waters, deeper into the mixed layer. Smith (1992) provides strong observational evidence for the mixing prowess of Langmuir circulation, while Li et al. (1995) were the first to incorporate them in ocean models and question their role in deepening the mixed layer. Other mechanisms have, of course, been proposed for deepening the mixed layer, of which a resonant interaction between Langmuir circulation and internal waves is perhaps the most robust theoretically (Chini and Leibovich, 2003). But it is a construct more suited to the next generation

of dynamic interactive sub-grid models, rather than the simple parametric models considered here and was thus not included in our study.

The need for coupling of small-scale and large-scale models has already been recognized by the oceanographic community. Qiao et al. (2004, 2008) suggested the coupling of wave models with ocean circulation models. In these studies, the waves were modelled explicitly, and the respective stresses were then input into the ocean models. Dramatic improvements were achieved in predicting the surface temperature, upper-ocean thermal structure and mixed-layer depth compared to the traditional mixing schemes.

In this paper, we did not intend to model the future changes to the climate as such and to explicitly quantify climate impacts of the wave-induced mixing of the upper-ocean. Rather, we show the differences in climate model outcomes with and without the wave mixing taken into account. Our main purpose is to demonstrate that an important physical mechanism, that is the ocean mixing due to waves, is presently missing in the climate models, whereas the effect of this mixing is significant.

Modelling the surface waves at the climate-change time scale is not always feasible, and in the present paper effects of the wave-induced upper-ocean mixing were parameterized in terms of the global winds. The parameterisations are discussed in Section 2. These also include a dependence for the synoptic wind gustiness, necessary to link the global winds with surface wave-generating winds. The wave-induced variable MLD is then incorporated into the climate model of intermediate complexity CLIMBER-2 (Ganopolski et al., 1998; Petoukhov et al., 2000). In Section 3, modelling of the pre-industrial climate is carried out, comparisons with available MLD data are conducted, and impacts on the simulation of spatial distributions and seasonal variations of the global atmospheric temperature, pressure and precipitation are analysed. In Section 3.3, future scenarios are modelled and differences due to the new features are highlighted. Section 4 provides discussion and conclusions.

## 2. Parameterisation of the mixed-layer depth in terms of the global wind

As mentioned in Section 1, the wind-generated waves and turbulence induced by such waves play a primary role in the mixing of the upper-ocean. There are three main wave-related physical mechanisms which, separately or together, can be held responsible for such mixing: injecting of turbulence in the course of wave breaking, direct generation of turbulence by the wave orbital motion and vertical circulation of the mixed-layer turbulence within Langmuir cells.

Significance of the first mechanism is universally recognized and is possibly exaggerated as discussed below in Section 4. Since the turbulence due to wave breaking is only plunged in near the surface, various mixing schemes are employed in general circulation models (GCMs) in order to diffuse this turbulence down and thus produce the upper-ocean mixing in absence of vertical convection (i.e.  $k - L$  and  $k - \epsilon$  models of oceanic turbulence, see, for example, Craig (2005)). The other two mechanisms, produced or triggered by the waves, either generate turbulence directly throughout the water column, or facilitate its downward transport. Since modelling the waves within a climate model is not feasible at this stage, in the present paper MLD due to these two processes will be parameterized.

Relative importance of the three mechanisms is not clear as dedicated experimental comparisons are not available. Each of them separately has been claimed to be able to explain observed values of MLD. In the current study, the two non-breaking wave-induced mixings will be considered independently.

## 2.1. Wave-induced non-breaking turbulence

While the turbulence injected by breaking waves is commonly perceived as one of the main means to transfer wind momentum into subsurface waters and has been broadly implemented in ocean-circulation and ocean-mixing models (Craig, 2005), the notion of a non-breaking wave-induced turbulence is a relatively new concept, although it has been foreshadowed in a number of experimental (Yefimov and Khristoforov, 1971; Cavaleri and Zecchetto, 1987; Gemmrich and Farmer, 2004; Babanin et al., 2005; Gemmrich, submitted for publication), theoretical (Thais and Magnaudet, 1996; Phillips, 2001; Arduin and Jenkins, 2006) and numerical studies (Pleskachevsky et al., 2001, 2005; Qiao et al., 2004, 2008; Gayer et al., 2006).

The physical concept of the turbulence induced directly by non-breaking waves was originally suggested by Babanin (2006) as a hypothesis of wave-amplitude-based Reynolds number

$$Re = \frac{a^2 \omega}{\nu}, \quad (1)$$

which is meant to indicate a transition from laminarity to turbulence for the wave orbital motion. Here,  $a$  is the wave amplitude (radius of the wave orbit) at the surface,  $\omega$  is the angular frequency and  $\nu$  is the kinematic water viscosity. Estimates of the critical wave Reynolds number provided an approximate value of  $Re_{cr} = 3000$ , and various comparisons were conducted to verify this threshold. In particular, once this number was used for ocean conditions (where mixing due to heating and cooling is less important than that due to the waves) quantitative and qualitative characteristics of the ocean's MLD were shown to be predicted with a good degree of agreement with observations.

The phenomenon was further investigated in a laboratory experiment (Babanin and Haus, 2009). Wavenumber velocity spectra beneath surface waves of different steepnesses, in absence of wave breaking, were measured. While intermittent, they exhibited the Kolmogorov interval associated with the presence of isotropic turbulence. Magnitudes of the energy dissipation rates due to this turbulence in the particular case of 1.5 Hz deep-water waves were quantified as a function of the surface wave amplitude. The dependence conformed with the expectation that, since the force due to the turbulent stresses is proportional to  $a^2$ , the energy dissipation rate should be  $\sim a^3$ .

According to Babanin (2006), the depth of the mixed layer  $z_{cr}$  due to the wave-induced turbulence should be

$$z_{cr} = \frac{g}{2\omega^2} \ln \frac{a^2 \omega}{Re_{cr} \nu}, \quad (2)$$

where  $g$  is the gravitational constant. For spectral waves, the surface wave amplitude can be represented approximately by half the significant wave height,  $H_s$ , implying  $a = H_s/2$ , and by the peak wave frequency  $\omega_p$ .

Wave height  $H_s$  and peak frequency  $\omega_p$ , however, are sub-grid properties in CLIMBER. Their estimates were obtained by employing the Pierson–Moscowitz (PM) limit for fully developed waves (Pierson et al., 1964), i.e. connection of the wave height and peak frequency of the fully developed waves with the surface wind speed at 10-m height  $U$ :

$$\tilde{f}_p^{PM} = \frac{f_p^{PM} U}{g} \approx 0.13, \quad (3)$$

$$\tilde{m}^{PM} = \frac{g^2 m^{PM}}{U^4} \approx 2.7 \cdot 10^{-3}. \quad (4)$$

Here,  $f_p = \omega_p/(2\pi)$  and  $m$  is wave variance:  $H_s = 4\sqrt{m}$ . Therefore, the final expressions for  $\omega$  and  $a$  to be substituted in (2) are:

$$\omega = 0.82 \frac{g}{U}, \quad (5)$$

$$a = 0.12 \frac{U^2}{g}. \quad (6)$$

Since these are characteristics of waves at their ultimate stage of development, Eq. (5) is a lower frequency limit whereas Eq. (6) is the upper amplitude limit. Real waves are rarely at full development, but in the open ocean they are usually well-developed for practical purposes. Given other uncertainties in the model, and in particular the link between global winds and surface wind-generating winds (see Section 2.3 below), Eqs. (2), (5) and (6) should provide a reasonable approximation of the wave-induced MLD in terms of the wind speed. Kinematic viscosity  $\nu$  of the sea water, with three significant digits of precision, can be calculated as following:

$$\nu = ((0.659 \cdot 10^{-3} \cdot (T - 1) - 0.05076)(T - 1) + 1.7688) \cdot 10^{-6} \quad (7)$$

where  $T$  is the surface temperature in degrees of Celcius (the formula is taken from [http://ittc.sname.org/2002\\_recomm\\_proc/7.5-02-01-03.pdf](http://ittc.sname.org/2002_recomm_proc/7.5-02-01-03.pdf)).

## 2.2. Langmuir circulation

Langmuir circulation is triggered by an instability excited by the interaction of a wave field both with itself and with a sheared, usually wind induced, current (Craik and Leibovich, 1976; Phillips, 1998). Once formed, however, Langmuir circulation can persist in the absence of wind (Craik, 1982; Plueddemann et al., 1996; Phillips, 2002) but it cannot persist in the absence of waves and is thus a wave-related phenomenon (see e.g. Smith, 1992; Phillips, 2001, 2003, 2005). Therefore, in the context of the present study, our intent is to parameterise Langmuir circulation in the same general terms as wave-induced mixing.

Langmuir circulation typically forms in tens of minutes in winds above 3 m/s and can grow to spacings in excess of one kilometer and to depths circa 100 m (Thorpe, 2004). They have thus long been considered a means to form the mixed layer (Langmuir, 1938) and observations bear this out (Smith, 1992). They are also thought to deepen the mixed layer (Li et al., 1995), particularly during storms. Nevertheless, because they cover only 15–20% of the ocean surface at any time they are necessarily secondary to the ubiquitous upper-ocean mixing caused by wind-generated seas.

Field observations of mixed layer formation due to Langmuir circulation are rare, but Smith (1992, 1998) gives detailed accounts of such, both in moderate winds and seas and during a storm. In each instance the depth of the mixed layer scaled with the wavelength of the dominant-slope surface waves, thereby suggesting the relationship

$$z_{LC} = A \frac{U^2}{g}. \quad (8)$$

To render (8) useful for our calculations, the constant  $A$  was chosen to match Smith's (1992) observations in which waves of 25 m length are present in 8 m/s winds, suggesting that  $A = 4$ . Note that Langmuir circulation were not observed until the wind freshened to 13 m/s but there was no immediate change in the wavelength of the waves.

Dependencies (2) and (8) are compared in Fig. 1. Over the range of wind speeds shown, parameterisation (8) is a weaker function of the wind speed and, if taken alone, is likely to underestimate the average MLD. For example, for wind speeds of 10 m/s, which is close to average extra-tropical values, the wave-induced MLD

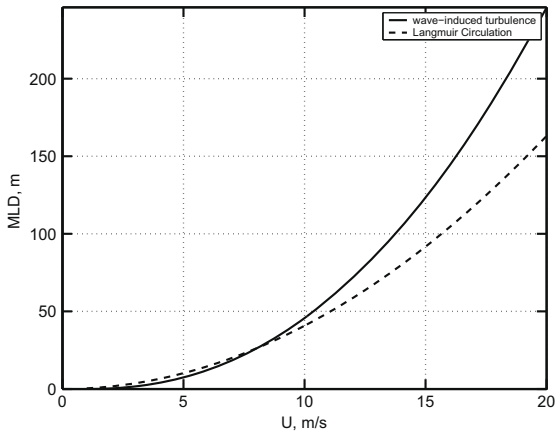


**Fig. 1.** Prediction of MLD as a function of wind speed  $U$ , assuming that the mixing is driven either by the wave turbulence only (solid line) or by Langmuir circulation only (dashed line).

formula (2) produces average depths just under 50 m which is in reasonable agreement with observations (Carton et al., 2008) while Langmuir-circulation dependence (8) suggests a MLD of about 40 m. Therefore surface mixing as a consequence of wave-induced turbulence should, on average, dominate. And, although Langmuir circulation may act locally over smallish time scales, days or weeks say, to deepen the mixed layer, the long-term average resulting solely from wave-induced turbulence is essential. Indeed, if, for example, the global winds were to grow to reach 15 m/s, the mixing by wave-induced turbulence would realise a 125 m-deep MLD and thus significantly alter the ocean–atmosphere thermodynamic balance.

### 2.3. The issue of global-wind gustiness

It is important to recognize that the global geostrophic winds, generated by the climate model, and the surface wave-generating winds are not the same. If the geostrophic winds are used to predict MLDs, parameterized in terms of the surface winds, underestimation may be as large as a factor of two (Ganopolski, 1998). This is due to the gustiness of geostrophic winds.

Anomalies of the magnitude of the surface winds with respect to mean values associated with geostrophic winds are well-known (e.g. Serra et al., 2002). It is apparent that deepening of the mixed layer is conducted when excessive deviations from the mean occur, provided they are sufficiently long for MLD to settle (normally tens of hours (e.g. Martin, 1985)). Extremely strong anomalies (for example, hurricanes or severe storms where the wind magnitudes are significantly greater than average) are usually localized to a relatively small area and rarely persist that long in one location, and therefore will have no noticeable impact on the ocean’s MLD at large-scale.

The anomalies of interest are those which can be described as gustiness of the wind at synoptic time scales. Physical models for such gustiness, tested in a regional climate model, are now available (Brasseur, 2001; Stephane et al., 2003). According to the Brasseur model, speed of the wind gusts at this scale depends on the large-scale winds and structure of the atmospheric boundary layer, including its turbulence and stability. Physical modelling of the gustiness by means of the Canadian regional climate model (Stephane et al., 2003) demonstrated that well-resolved topography is also important.

Information on the turbulent structure of the boundary layer and on the topography is not available within the model of intermediate complexity used in the present study, and therefore the

physical model cannot be directly employed. Unfortunately, to the best of our knowledge, explicit parameterisations for wind gustiness at synoptic scales are not available either. Therefore, in this paper, dependence of maximal gustiness on the mean wind speed was adopted from the small-scale atmospheric turbulence by analogy, and representative extreme surface winds are estimated from the mean global winds as following (Babanin and Makin, 2008):

$$U_{max} = U_{mean} + 0.60 \cdot U_{mean}^{0.29}. \quad (9)$$

Since the impact of global wind gustiness is essential in determining wave-generating winds, then the waves and ultimately the upper-ocean mixing (e.g. Ganopolski, 1998), the gustiness parameterisation (9) is used throughout in this paper. We realise, however, the difference between the two-dimensional large-scale isotropic turbulence and the three-dimensional small-scale isotropic turbulence and the need to rectify this expression once the necessary experimental data become available. In GCMs, this technicality can be by-passed by using the physical model of Brasseur (2001) for the gustiness.

### 2.4. Introducing the variable MLD in CLIMBER-2 model

To study the effect of variable mixed-layer depth on simulated equilibrium climate state and climate change, we use the climate model of intermediate complexity CLIMBER-2 (Ganopolski et al., 1998; Petoukhov et al., 2000). Standard version of the CLIMBER-2 model is denoted hereafter as “STD”. It has fixed 50 m MLD, i.e. it does not depend on wind or waves as the wave-induced MLD shown in Fig. 1. The version of CLIMBER-2 which includes variable mixed layer is called “VMD”.

If compared to the state-of-art climate models, CLIMBER-2 has a rather coarse spatial resolution and a number of processes in the ocean and the atmosphere are significantly simplified. In particular, the atmospheric component of the model is represented by a statistically-dynamical atmosphere model which has latitudinal resolution of  $10^\circ$  and longitudinal resolution of  $51.4^\circ$ . Different modules of atmospheric model have different vertical resolution. For example, radiation scheme employs 16 vertical levels whilst atmospheric dynamics is computed on 10 levels. The ocean component of the model is based on the zonally averaged ocean model similar to that of Wright and Stocker (1991), and in the longitudinal direction it only resolves three major oceanic basins (Pacific, Atlantic and Indian) while in latitudinal direction it has  $2.5^\circ$  resolution and vertically the ocean is divided by 21 uneven levels. The oceanic component uses a simple diagnostic equation for calculation of meridional overturning circulation rather than a complete set of momentum equations. At the same time, it was shown that the CLIMBER-2 model is not only able to reproduce the modern climate state quite realistically, but also has a sensitivity to different climate forcings such as  $CO_2$ , solar constant, freshwater flux, consistent with that of the state-of-art climate models (Ganopolski et al., 2001; Petoukhov et al., 2005; Rahmstorf et al., 2005). It is also noteworthy that the treatment of the oceanic thermodynamics is essentially the same in CLIMBER-2 as in the 3-D oceanic GCMs. Obviously, the main advantage of CLIMBER-2 is its fast turnaround time which allows one to perform many long runs required to attain fully equilibrium climate state and to test the model’s sensitivity. Moreover, apart from the lack of longitudinal resolution, oceanic component of CLIMBER-2 has essentially the same latitudinal and vertical resolutions as the oceanic components of coupled GCMs used for long-term simulations and climate predictions. Therefore, one can expect that results obtained with CLIMBER-2, at least qualitatively, are also applicable to realistic climate models.

Incorporation of the variable MLD into the  $z$ -coordinate ocean models represents a considerable challenge. Here, we employ a somewhat simplified approach based on a two-step solution for the tracer equations. At the first step, new values for temperature (salinity) were computed at the standard  $z$ -coordinate grid using FCT (flux corrected transport) numerical scheme for the advection of tracers and second order scheme for the diffusion. Then using MLD ( $h$ ) computed by Eq. (2) or (8), temperature (salinity) of ML was computed and temperatures (salinities) at the  $z$ -coordinate grid were recalculated (see below) to enforce energy (salinity) conservation. In fact, two different situations are possible in the model. The first case is MLD being smaller than the depth of the uppermost model layer  $z_1 = 50$  m. In this case, simulated ML temperature (salinity) does not affect temperatures (salinity) at  $z$ -grid directly. It affects, however, temperatures indirectly, by determining the surface heat flux. This is because in the model version with variable MLD the sea surface temperature used for calculations of the sensible and latent heat fluxes is set to the ML temperature rather than to the temperature of the uppermost  $z$ -level, like in the standard model version. In the second case of  $h > z_1$ , temperature (salinities) at all  $z$ -levels above the bottom of ML were set to that computed for ML.

The equation for ML temperature (similar equation is used for salinity) is

$$c\rho h \frac{\partial T_m}{\partial t} = F_s - F_h + Q_{had}, \quad (10)$$

where  $c$  is the specific heat capacity of water,  $\rho$  is water density,  $F_s$  is the net heat flux through the ocean surface and  $F_h$  is the heat flux at the bottom of ML computed as

$$F_h = \kappa \frac{T_m - T_h}{\Delta z_n} + c\rho F_{ent}, \quad (11)$$

where the first term on the right-hand side of Eq. (11) represents vertical diffusive flux through the bottom of the ML with the vertical diffusivity  $\kappa = 0.310^{-4} \text{m}^2/\text{s}$ , the same as the background vertical diffusivity used in the model for all tracers in the upper 1 km of the ocean,  $T_h$  is the temperature below ML and  $\Delta z_n$  is thickness of the  $n$ -th model layer in which the bottom of ML is currently located. The second term,  $F_{ent}$  represents the so-called ‘‘entrainment flux’’:

$$F_{ent} = \begin{cases} (T_m - T_h) \left( \frac{\partial h}{\partial t} - w_h \right) & \text{for } \frac{\partial h}{\partial t} > w_h, \\ 0 & \text{for } \frac{\partial h}{\partial t} < w_h, \end{cases} \quad (12)$$

where  $w_h$  represents the vertical velocity at the bottom of ML. In the model, it is computed by interpolating between two neighboring model levels. Lastly, the term  $Q_{had}$  represents the convergency (divergency) of the horizontal heat flux associated with horizontal advection and diffusion. For simplicity, it was assumed that the convergency (divergency) of horizontal heat flux per unit of volume is constant within each horizontal model layer and hence

$$Q_{had} = \begin{cases} \frac{h}{\Delta z_1} A_1 & \text{if } h < z_1, \\ \sum_{i=1}^{n-1} A_i + \frac{h - z_{n-1}}{\Delta z_n} A_n & \text{if } z_{n-1} < h < z_n, \end{cases} \quad (13)$$

where  $A_i$  is the vertically integrated convergency (divergency) of the horizontal heat transport within the  $i$ -th model layer and  $z_i$  is the depth of the bottom of  $i$ -th layer. Temperature below the ML,  $T_h$  was computed from the conservation of energy in the vertical column. In the simplest case of  $h < z_1$ , the equation for  $T_h$  is:

$$T_h(z_1 - h) + T_m h = T_1 z_1. \quad (14)$$

For description of the deep wintertime convection, CLIMBER-2 employs a standard convective adjustment procedure which is activated when the simulated vertical density profile becomes unstable. In the case of convective adjustment, the depth of

the mixed layer is set to the depth of the bottom of the last layer involved in convective adjustment. In the grid-cells where the depth of convective ML is larger than that given by Eq. (2), ML module described by Eqs. (10)–(12) is disabled, and the model operates in its standard regime. Apart from introducing the variable mixed-layer depth, VMD version of the model is identical to the STD version.

### 3. Modelling pre-industrial climate

In this section we compare simulations of the equilibrium pre-industrial climate performed with the standard version (STD) of the CLIMBER-2 model with the version VMD which includes variable mixed-layer depth as described in the previous section. We performed two separate runs, each 3000 years long with constant preindustrial boundary conditions for variable mixed-layer depths described by Eqs. (2) and (8) respectively. In both cases, qualitative patterns of the change of the environmental characteristics were similar, but wave-induced MLD parameterisation (Eqs. (2), (5)–(7) and (9)) proved to be in a better agreement with the global atlas for monthly changes of the mixed-layer provided by the US Naval Research Laboratory (NRL) (<http://www7320.nrlssc.navy.mil/nmld/nmld.html>). Since this paper was mainly intended on investigation of influence of variable MLD on performance of CLIMBER-2, rather than on distinguishing between the two wave-mixing mechanisms, further comparisons and illustrations below are conducted for the wave-turbulence mixing parameterisation.

#### 3.1. Mixed-layer depth

Comparisons of the CLIMBER-2 results with the NRL atlas mixed layer depth are shown in Fig. 2. Panels in the figure indicate the latitudes 55 (a and b) and 35 (c and d) North, as the most effective wave-induced mixing (i.e. outside of tropical and arctic areas) is expected in these regions. Solid line represents the model, and dashed line the NRL atlas. Left panels correspond to the Atlantic Ocean, and right panels to the Pacific. Only summer months are shown as in winter the mixing is dominated by the vertical convection and is much deeper compared to the wind-wave-induced mixing, and CLIMBER-2 switches to the convective scheme as described in Section 2.4.

The model produces zonally averaged values of MLD for each of the ocean basins, and therefore for demonstrations longitudinal transects are chosen from the atlas values reasonably close to the centerline of the Pacific and Atlantic, i.e. 24° and 170° West correspondingly. The NRL atlas was ‘‘constructed from the 1° monthly-mean temperature and salinity climatologies of the World Ocean Atlas 1994 (Levitus and Boyer, 1994; Levitus et al., 1994) using a method for determining layer depth that can accommodate the wide variety of temperature and density profiles that occur within the global ocean’’ and is therefore a modelling outcome itself. Thus, the comparison in Fig. 2 is qualitative rather than direct. Given other uncertainties of the parameterisation mentioned in Section 2, agreements of the modelled and observed values are satisfactory: not only magnitudes of the mixed-layer depth are reasonably close, but also their seasonal trends are similar and maxima are located in reasonable proximity. Now that the model has a realistic variable behavior of MLD, both in winter and in other seasons, the importance of the newly introduced variations can be investigated.

#### 3.2. Impact of the variable MLD on global climate

In this Section, we analyse the impact of variations in MLD on the climatological characteristics simulated by CLIMBER-2 by

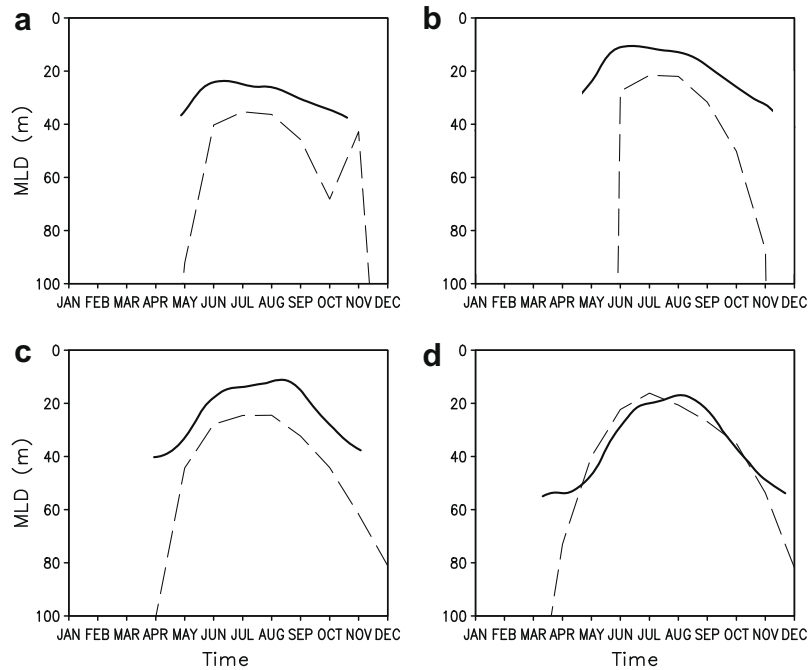


**Fig. 2.** Seasonal variations of MLD at 55 (a and b) and 35 (c and d) degrees of Northern latitude, zonally averaged. (left panels) Atlantic Ocean, (right panels) Pacific Ocean. Solid line represents the model, and dashed line NRL atlas. For the model, MLD is shown only for time interval when the wave-induced MLD is larger than convective MLD.

comparing the equilibrium pre-industrial climate state computed by means of the STD and VMD versions of the model. Interestingly, the differences between the STD and VMD version with respect to globally averaged surface air temperature, SST (sea surface temperature) and volume-averaged ocean temperature, are rather small (below 0.1 °C). Ocean overturning circulation is also essentially identical in two runs. Regional differences in annual mean surface air temperature are somewhat larger, but still less than 0.5 °C, and for most of the globe are also below 0.1 °C. Hence, introducing the time-dependent MLD does not change annual mean climate characteristics appreciably.

What has changed significantly, however, is the magnitude of seasonal variations of the global temperature at extra-tropical latitudes. In Fig. 3, seasonal variations zonally averaged over the World Ocean SST are shown at 25, 35, 45 and 55° North (from top to bottom correspondingly). In each panel, the thin line is produced with the STD version of CLIMBER, thick line with the VML and dashed line corresponds to observations (zonally averaged Levitus data).

At low latitudes (25° North in Fig. 3), the wave-induced mixing is weak as expected (e.g. Qiao et al., 2008) since the wind-generated waves in the tropics are small on average (e.g. Young and Holland, 1996). At higher latitudes, the wave-mixing effect is progressively increased and considerably improves agreement between simulated and observed SST if compared to STD version. Although the magnitude of seasonal SST variations at 55° is somewhat exaggerated compared to empirical data, encouraging in simulations at all latitudes is an improved phase relation between the model and observation, as the STD version appeared to lag behind the observational data.

The impact of variable MLD on simulated climate characteristics is illustrated in Fig. 4, which shows differences between VML and STD model versions for simulated summer (JJA) surface atmospheric temperature (top), sea-level pressure (middle) and precipitation (bottom). The impacts are obviously localized, and over the North Pacific the temperature differences between two model versions are as large as 3 °C. Since, during the warm season, the sim-

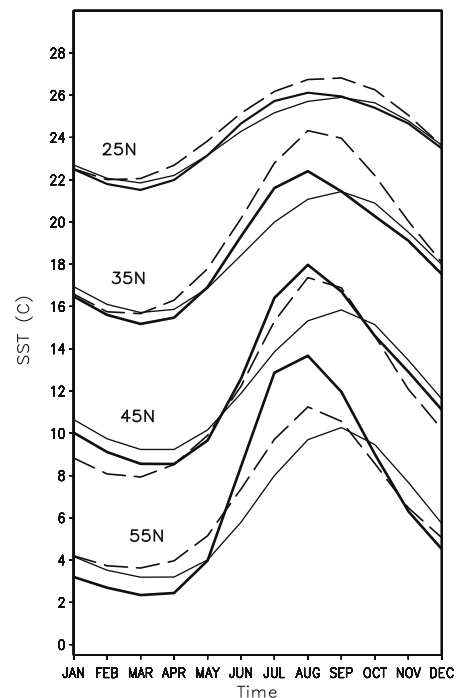


**Fig. 3.** Seasonal variations of the global zonally averaged SST. Panels shown: 25, 35, 45 and 55° North (from top to bottom). Lines shown: STD version of CLIMBER (thin), VML version (thick) and observations based on Levitus data (dashed).

ulated MLD is systematically smaller than the 50 m depth prescribed in the STD version, the summer hemisphere is systematically warmer while the winter hemisphere is colder in the VML version compared to STD. This enhances inter-hemispheric temperature difference which leads to a larger magnitude of poleward variations of the intertropical convergence zone (ITCZ), changes in the meridional and atmospheric circulation and monsoons.

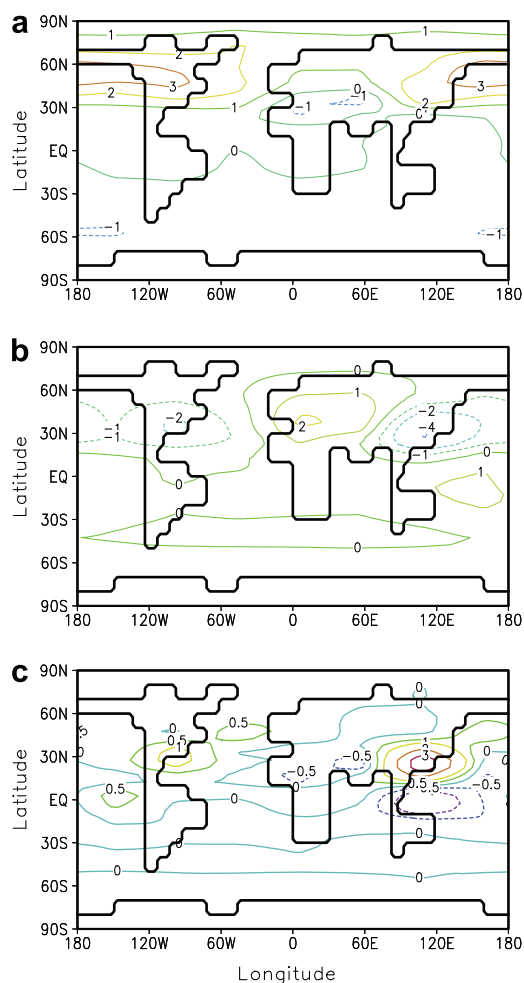


**Fig. 4.** Differences of summer (JJA) surface atmospheric temperature in degrees (a), sea-level pressure in mbar (b) and precipitation in mm per day (c) between VDM and STD model versions.

This is illustrated by Fig. 4b, which shows the difference between two model versions in the simulated sea level pressure field for the summer season. Introducing the variable MLD leads to a northward shift of ITCZ, lowering of SLP over Northern America and South Eastern Asia and an increase in SLP over North Africa and Central Asia. As a result (Fig. 4c), South Eastern Asian and North American monsoons are considerably stronger in the VML version, whilst North African and Indian monsoons are weaker. In addition, strengthening of South Eastern Asian monsoon leads to a significant reduction of precipitation in the equatorial region. Differences in summer precipitations between VML and STD reach in this region 3 mm/day which is almost 50% of the absolute value of precipitation simulated in STD version.

Fig. 5 shows seasonal evolution of the differences between two model versions in the global zonally averaged precipitation. It demonstrates that enhanced seasonality in the VML version has a rather symmetric impact on the hydrological cycle in both hemispheres, but the influence of variable MLD is stronger for the Northern Hemisphere which is primarily due to a stronger and less seasonally varying surface wind in the Southern Hemisphere.

Therefore, it can be concluded that introducing the variable MLD due to wave-induced mixing in CLIMBER-2 resulted in essential alterations to the amplitude of seasonal variations of the main meteorological properties compared to the standard model version. While globally averaged values of such alterations are signifi-

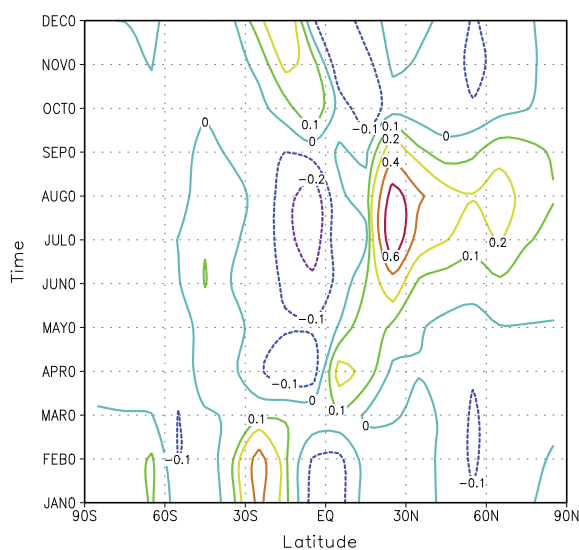


**Fig. 5.** Seasonal variations of the difference between VDM and STD model versions in zonally averaged precipitation.

cant, some localized effects are much greater and potentially bear essential environmental and social consequences.

At this stage, it should be noticed that introducing the variable mixed layer depth in CLIMBER-2 is also important for the general circulation models, not only for models of intermediate complexity which usually treat evolution of MLD in a rather simplistic manner. Since the direct wave-induced mixing is not accounted for by GCMs either, similar qualitative impacts on results of GCMs can be expected once their mixing schemes are updated to account for the wave effects. This is discussed in Section 4 below.

### 3.3. Climate response to CO<sub>2</sub> rise

To assess the role of variable MLD in simulation of the climate response to a continuous CO<sub>2</sub> concentration growth, we performed standard 100-year-long experiments with 1% per year increase of CO<sub>2</sub> concentration, with both model versions starting from corresponding equilibrium climate states. As far as the changes in globally averaged characteristics, such as globally averaged surface air temperature, SST, sea ice area, etc., as well as such characteristics like maximum of Atlantic meridional overturning, are concerned, differences between the STD and VML versions are very small. Hence, at least on the centennial time scale, details of ML parameterisations do not appear to affect appreciably transient mean annual climate response to the CO<sub>2</sub> rise. Nonetheless, for individual seasons and certain regions, differences between the two model versions in response to the CO<sub>2</sub> rise (i.e. after 70 years since the beginning of the numerical simulations) are not insignificant. For example, as it is shown in Fig. 6, the simulated changes in summer precipitation at the moment, when CO<sub>2</sub> is doubled, differ in some sensitive regions, such as South Eastern Asia, by up to 0.5 mm/day. This difference is comparable with the magnitude of precipitation change predicted by means of the default model for this region in case of the CO<sub>2</sub> doubling. In general, difference between the response of the two model versions to the CO<sub>2</sub> rise resemble the differences between the equilibrium simulations of pre-industrial climate state shown in Fig. 4c.

## 4. Discussion and conclusions

The results presented in this paper raise the issue of the importance of adequate modelling of the mixed-layer depth variation in

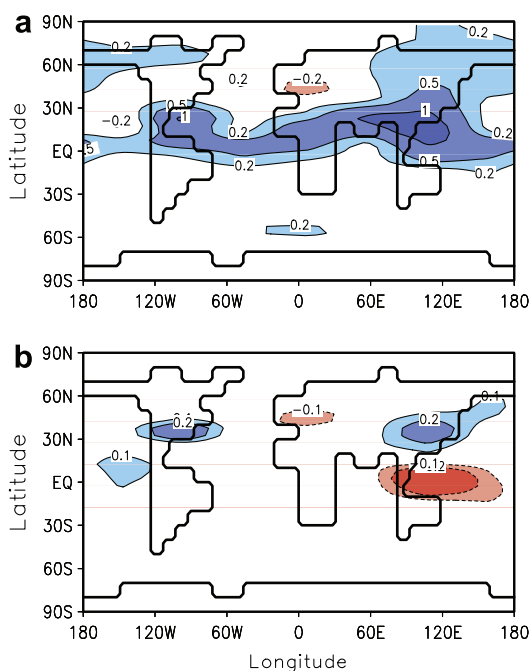


**Fig. 6.** Changes in summer (JJA) precipitation (mm/day) in STD model version (a) and difference in simulated precipitation changes between VML and STD (b) at the moment of CO<sub>2</sub> doubling.

climate models. In particular, emphasis is given to mixing driven directly by the waves, rather than through downward diffusion of the turbulence injected by wave breaking near the surface. The wave-induced mixing is simulated directly by introducing the variable mixed-layer depth in CLIMBER-2 model, compared to the standard version of the model which assumes the depth constant during the months when the vertical convection is not active. The variations are connected with parameterized properties of the waves and therefore the essential differences observed in the modelling outcomes should be attributed solely to such mixing.

In this regard, although simulations in the present paper are conducted by means of a model of intermediate complexity, the issue should be relevant for the general circulation ocean models (OGCMs) as well. Presently, the wave-induced mixing is not accounted for in such models, but if included it will provide an additional source of turbulent mixing. This should bring about alterations of the air-sea interactions similar to those observed in the model of intermediate complexity.

Indeed, although most of OGCMs do not simulate MLD explicitly, they implicitly require the uppermost model layer (or several upper layers) of the ocean to be well-mixed by means of the vertical turbulent mixing which is computed by using one of several existing mixing schemes. Although it seems to have automatically accounted for the upper-ocean mixing ultimately driven by the wind stress, there are a number of issues which do not appear well attended.

First, depending on the vertical resolution of OGCMs, this vertical mixing can be modelled accurately or crudely. Modern OGCMs used for climate modelling typically have 20–30 vertical levels, with the resolution in the upper 100 m of the ocean typically of 10–20 m. This is quite comparable with MLD over most of the World Ocean, at least, during the warm season. Therefore, the effective MLD in such models (one or several uppermost model layers) can considerably deviate from that in the real ocean.

Secondly, even if the vertical resolution of an OGCM is fine enough to make such an effect small, the mixing is still likely to be underestimated due to the disregard of the direct wave-induced

turbulence and circulation discussed in this paper. Indeed, out of the three wave-related mixing mechanisms: i.e. injection of turbulence in the course of wave breaking, direct generation of turbulence by the wave orbital motion and vertical circulation of the mixed-layer turbulence within Langmuir cells – only one is accounted for. And this one, the downward diffusion of the breaking turbulence, may probably appear the weakest of all.

Of course the wave breaking creates significantly enhanced levels of turbulence near the surface, compared to the case of non-breaking waves (e.g. Terray et al., 1996; Babanin et al., 2005). This effect ends, however, at the depths comparable with the wave height. Experimental evidence of the downward diffusion of such turbulence are not overwhelming. Vertical profiles of the volumetric rate of turbulent energy dissipation  $\epsilon$  decay rapidly as a function of distance  $z$  from the surface, i.e. as  $\epsilon \sim z^{-2}$  in the presence of breaking waves, and soon merge with values of dissipation rates which occur in the absence of wave breaking, i.e. described by profiles  $\epsilon \sim z^{-1}$  (Babanin et al., 2005).

Moreover, a relevant question in regard of the downward diffusion of the wave-breaking turbulence is its decay life. From general physical considerations, this is the order of seconds or even a fraction of a second. Can such turbulence survive the journey down to the bottom of the mixed layer if its mixing time scale is of the order of tens of hours (e.g. Martin, 1985)? Unlike pollutants, salinity and temperature, which will be eventually mixed in even if it takes years, the turbulence will simply dissipate.

Thus, the discussion highlights again the importance of wave-related physics in the upper-ocean. At the very least, Langmuir circulation should facilitate the mixing by providing the vertical advection to the surface-breaking turbulence. Although with the velocities of the order of cm/s, such advection may still be too slow for the smaller scale turbulence to survive. And in this regard, the wave-induced turbulence which can be directly generated at any depth where the wave motion is significant can turn a most important mechanism in the mixing.

MLD due to wave-induced mixing was introduced and parameterized in terms of the winds generated within the climate model of intermediate complexity CLIMBER-2. Within such models, parameterization of the wind gustiness is also an essential element, which in GCMs can be addressed explicitly by physical modelling of the gusts at synoptical scales. Obviously, such parameterizations can only be effective in ocean areas dominated by wind-generated waves, rather than swell. These effects were then tested, both for pre-industrial climate and in future scenarios. It is shown that seasonal variations of SST are rather sensitive to the MLD, and that introduction of a wind-induced parameterization for MLD improves agreement between modelling results and empirical data in circumstances when the wave-induced mixing is expected to be most significant. Moreover, the variable MLD considerably affects atmospheric dynamics and precipitation fields, especially on seasonal time scale. Apart from that, MLD and its seasonal variations are also important for modelling the oceanic carbon cycle, especially, its biological component. Therefore, adequate/accurate modelling of MLD is crucial for improvements of the climate model performance in simulation of modern climate and future climate change.

## References

- Arduini, F., Jenkins, A.D., 2006. On the interaction of surface waves and upper ocean turbulence. *J. Phys. Oceanogr.* 36, 551–557.
- Babanin, A.V., Young, I.R., Mirfenderesk, H., 2005. Field and laboratory measurements of wave-bottom interaction. In: Townsend, M., Walker, D. (Eds.), *Proc. 17th Australasian Coastal and Ocean Engineering Conf. and 10th Australasian Port and Harbour Conf.*, 20–23 September 2005, Adelaide, South Australia. The Institution of Engineers, Canberra, Australia, pp. 293–298.
- Babanin, A.V., 2006. On a wave-induced turbulence and a wave-mixed upper ocean layer. *Geophys. Res. Lett.* 33, L20605. doi:10.1029/2006GL027308.

- Babanin, A.V., Makin, V.K., 2008. Effects of wind trend and gustiness on the sea drag: Lake George study. *J. Geophys. Res.* 113, C02015. doi:10.1029/2007JC004233.
- Babanin, A.V., Haus, B.K., 2009. On the existence of water turbulence induced by non-breaking surface waves. *J. Phys. Oceanogr.* in press.
- Brasseur, O., 2001. Development and application of a physical approach to estimating wind gusts. *Mon. Weather Rev.* 129, 5–25.
- Carton, J.A., Grodsky, S.A., Liu, H., 2008. Variability of the oceanic mixed layer. *J. Climate* 21, 1029–1047.
- Cavaleri, L., Zecchetto, S., 1987. Reynolds stresses under wind waves. *J. Geophys. Res.* C92, 3894–3904.
- Chini, G.P., Leibovich, S., 2003. Resonant Langmuir-circulation-internal-wave interaction. Part 1. Internal wave reflection. *J. Fluid Mech.* 495, 35–55.
- Craig, P.D., 2005. In: Baumert, H., Simpson, J., Sundermann, J. (Eds.), *Marine Turbulence – Theories, Observation and Models*. Cambridge University Press, Cambridge, UK, p. 76p.
- Craik, A.D.D., Leibovich, S., 1976. A rational model for Langmuir circulations. *J. Fluid Mech.* 73, 401–426.
- Craik, A.D.D., 1982. The drift velocity of water waves. *J. Fluid Mech.* 116, 187–205.
- Donelan, M.A., 1990. Air–sea interaction. *Sea: Ocean Eng. Sci.* 9, 239–292.
- Donelan, M.A., 1998. Air–water exchange processes. In: Imberger, J. (Ed.), *Physical Processes in Lakes and Oceans*, vol. 54. Coastal and Estuarine Studies, AGU, pp. 19–36.
- Ganopolski, A., 1998. The role of synoptic variability of wind velocity in formation of the vertical thermal structure in the ocean upper layer. *Morskoi Gidrofizicheskii Zhurnal* 6, 23–28 (in Russian, English abstract).
- Ganopolski, A., Rahmstorf, S., Petoukhov, V., Claussen, M., 1998. Simulation of modern and glacial climates with a coupled global model of intermediate complexity. *Nature* 351, 351–356.
- Ganopolski, A., Petoukhov, V., Rahmstorf, S., Brovkin, V., Claussen, M., Eliseev, A., Kubatzki, C., 2001. CLIMBER-2: a climate system model of intermediate complexity. Part II: model sensitivity. *Clim. Dynam.* 17, 735–751.
- Gayer, G., Dick, S., Pleskachevsky, A., Rosenthal, W., 2006. Numerical modeling of suspended matter transport in the North Sea. *Ocean Dyn.* 56, 62–77.
- Gemmrich, J.R., Farmer, D.M., 2004. Near-surface turbulence in the presence of breaking waves. *J. Phys. Oceanogr.* 34, 1067–1086.
- Gemmrich, J.R., submitted for publication. Turbulence beneath young waves. *J. Phys. Oceanogr.*
- Gill, A.E., 1982. *Atmosphere–Ocean Dynamics*. Elsevier. 662p.
- Kudryavtsev, V.N., Makin, V.K., 2002. Coupled dynamics of short waves and the airflow over long surface waves. *J. Geophys. Res.* C107, 3209. doi:10.1029/2001JC001251.
- Langmuir, I., 1938. Surface motion of water induced by the wind. *Science* 87, 119–123.
- Levitus, S., Burgett, R., Boyer, T.P., 1994. *World Ocean Atlas 1994. Salinity*. NOAA Atlas NESDIS 3, US Govt. Print. Off., Washington, DC, 99p.
- Levitus, S., Boyer, T.P., 1994. *World Ocean Atlas 1994. Temperature*. NOAA Atlas NESDIS 4, US Govt. Print. Off., Washington, DC, 117p.
- Li, M., Zahariev, K., Garrett, C., 1995. Role of Langmuir circulation in the deepening of the ocean surface mixed layer. *Science* 270, 1955–1957.
- Martin, P.J., 1985. Simulation of the mixed layer at OWS November and Papa with several models. *J. Geophys. Res.* C90, 903–916.
- McWilliams, J.C., Sullivan, P.P., Moeng, C.-H., 1997. Langmuir circulations in the ocean. *J. Fluid Mech.* 334, 1–30.
- Petoukhov, V., Ganopolski, A., Brovkin, V., Claussen, M., Eliseev, A., Kubatzki, C., Rahmstorf, S., 2000. CLIMBER-2: a climate system model of intermediate complexity. Part I: model description and performance for present climate. *Clim. Dynam.* 16, 1–17.
- Petoukhov, V., Claussen, M., Berger, A., Crucifix, M., Eby, M., Eliseev, A.V., Fichefet, T., Ganopolski, A., Goosse, H., Kamenkovich, I., Mokhov, I.I., Montoya, M., Mysak, L.A., Sokolov, A., Stone, P., Wang, Z., Weaver, A.J., 2005. EMIC Intercomparison Project (EMIP CO2): comparative analysis of EMIC simulations of climate, and of equilibrium and transient responses to atmospheric CO2 doubling. *Clim. Dynam.* 25, 363–385. doi:10.1007/s00382-005-0042-3.
- Phillips, W.R.C., 1998. Finite amplitude rotational waves in viscous shear flows. *Stud. Appl. Math.* 101, 23–47.
- Phillips, W.R.C., 2001. On an instability to Langmuir circulation and the role of Prandtl and Richardson numbers. *J. Fluid Mech.* 442, 335–358.
- Phillips, W.R.C., 2002. Langmuir circulation beneath growing or decaying surface waves. *J. Fluid Mech.* 469, 317–342.
- Phillips, W.R.C., 2003. Langmuir circulation. In: Sajjadi, S.G., Hunt, J.C.R. (Eds.), *Wind Over Waves II: Forecasting and Fundamentals of Applications*. Horwood Publishing, Chichester, UK, pp. 157–167.
- Phillips, W.R.C., 2005. On the spacing of Langmuir circulation in strong shear. *J. Fluid Mech.* 525, 215–236.
- Pierson Jr., W.J., Moskowitz, L., 1964. A proposed spectral form for fully developed wind seas based on the similarity theory of S.A. Kitaigorodskii. *J. Geophys. Res.* 69, 5181–5190.
- Pleskachevsky, A., Hoststman, J., Rosenthal, W., 2001. Modeling of sediment transport in synergy with ocean color data. In: Proc. 4th Berlin workshop on ocean remote sensing, Wissenschaft und Technik Verlag, Berlin, 30 May–01 June 2002, pp. 177–182.
- Pleskachevsky, A., Gayer, G., Hoststman, J., Rosenthal, W., 2005. Synergy of satellite remote sensing and numerical modeling for monitoring of suspended particulate matter. *Ocean Dyn.* 55, 2–9.
- Plueddemann, A.J., Smith, J.A., Farmer, D.M., Weller, R.A., Crawford, W.R., Pinkel, R., Vagle, S., Gnanadesikan, A., 1996. Structure and variability of Langmuir circulation during the Surface Waves Processes Program. *J. Geophys. Res.* 101, 3525–3543.
- Qiao, F., Yeli, Y., Yang, Y., Zheng, Q., Xia, C., Ma, J., 2004. Wave-induced mixing in the upper ocean: distribution and application to a global ocean circulation model. *Geophys. Res. Lett.* 31, L11303. doi:10.1029/2004GL019824.
- Qiao, F., Yang, Y., Xia, C., Yeli, Y., 2008. The role of surface waves in the ocean mixed layer. *Acta Oceanol. Sin.* 27, 30–37.
- Rahmstorf, S., Crucifix, M., Ganopolski, A., Goosse, H., Kamenkovich, I., Knutti, R., Lohmann, G., Marsh, R., Mysak, L.A., Wang, Z., Weaver, A.J., 2005. Thermohaline circulation hysteresis: a model intercomparison. *Geophys. Res. Lett.* 32, L23605. doi:10.1029/2005GL023655.
- Serra, Y.L., Houze Jr., R.A., 2002. Observations of variability on synoptic time scales in the East Pacific ITCZ. *J. Atmos. Sci.* 59, 1723–1743.
- Smith, J., 1992. Observed growth of Langmuir circulation. *J. Geophys. Res.* 97, 5651–5664.
- Smith, J., 1998. Evolution of Langmuir circulation in a storm. *J. Geophys. Res.* 103, 12649–12668.
- Soloviev, A., Lukas, R., 2006. *The Near-surface Layer of the Ocean: Structure Dynamics and Applications*. Springer. 572p.
- Stephane, S., Brasseur, O., Beniston, M., 2003. Application of a new wind gust parameterization: multiscale case studies performed with the Canadian regional climate model. *J. Geophys. Res.* D108. doi:10.1029/2002JD002646.
- Terray, E.A., Donelan, M.A., Agrawal, Y.C., Drennan, W.M., Kahma, K.K., Williams III, A.J., Hwang, P.A., Kitaigorodskii, S.A., 1996. Estimates of kinetic energy dissipation under breaking waves. *J. Phys. Oceanogr.* 26, 792–807.
- Thais, L., Magnaudet, J., 1996. *J. Fluid Mech.* 328, 313–344.
- Thorpe, S.A., 2004. Langmuir circulation. *Annu. Rev. Fluid Mech.* 36, 55–79.
- Wright, D.J., Stocker, T.F., 1991. A zonally averaged ocean model for the thermohaline circulation. Part I: model development and flow dynamics. *J. Phys. Oceanogr.* 21, 1713–1724.
- Yefimov, V.V., Khristoforov, G.N., 1971. Spectra and statistical relations between the velocity fluctuations in the upper layer of the sea and surface waves. *Izv., Atmos. Ocean. Phys.* 7, 1290–1310.
- Young, I.R., Holland, G.J., 1996. *Atlas of the Oceans: Wind and Wave Climate*. Pergamon Press, ISBN 0-08-042519-4. 241p.